10th World Congress on Structural and Multidisciplinary Optimization
May 19 - 24, 2013, Orlando, Florida, USA

Multiscale Topology Optimization of Structures and Non-Periodic Cellular Materials

Kai Liu[1], Kapil Khandelwal[2], Andrés Tovar[1]

[1]Department of Mechanical Engineering
Indiana University-Purdue University Indianapolis, Indianapolis, IN 46202, USA
Emails: kailiu@iupui.edu,tovara@iupui.edu
[2]Department of Civil & Environmental Engineering & Earth Sciences
University of Notre Dame, Notre Dame, IN 46556, USA
Email: kapil.khandelwal@nd.edu

1. Abstract
Topology optimization allows designers to obtaining lightweight structures considering the binary distribution of a solid material. Further material savings and increased performance may be achieved if the material and the structure topologies are concurrently optimized. The use of homogenization methods promotes the introduction of material-scale parameters in the problem's formulation. While some research has been focused on material parameters and periodic topology optimization, this work deals with non-periodic material topologies. Since no preconceived material and structure geometries are considered, the multiscale approach is capable of driving the design to innovative and potentially better configurations at both length scales. The proposed methodology is applied to minimum compliance problems and compliant mechanism synthesis. The multiscale results are compared with the traditional structural-level designs in the context of Pareto solutions, demonstrating benefits of ultra-lightweight configurations.
2. Keywords: hierarchical, homogenization, multiscale, non-periodic, topology optimization

3. Introduction
Topology optimization is a design method used to find optimal material distribution within a design domain. For a given set of boundary and loading conditions, topology optimization drives the material distribution process to a structural layout that maximizes performance objectives and satisfies design constraints. Traditionally, lightweight concept designs have been obtained using homogeneous materials. However, this approach is challenged by the use of cellular materials. The use of cellular materials in topology optimization results on multiscale arrangements are referred to as ultra-lightweight structures. Ultra-lightweight structures are characterized by a high strength-to-weight ratio, and are desired in automobile, aerospace, and aircraft design due to their high performance and reduced energy consumption involved. Cellular materials are commonly selected from a set of commercially available layouts, e.g., triangular, cubic, and honeycomb among others.
Topology optimization in cellular materials design acts for an important alternative to classic materials design procedures. The structural design is closely related to the design of meso-structural cellular materials via the direct homogenization theory [1, 2]. In contrast, the inverse homogenization is a topology optimization procedure, which denotes to obtain material distribution of micro-/meso-scale with desired homogenized or effective material properties. Since it has been proposed by Sigmund [3], the inverse homogenization method has been applied for numerous different applications, such as material with negative Poisson's ration [3], Functionally Graded Materials (FGM), which are continuously graded in one or more specified directions [4], and has been adapted for multi-functional composites design (c.f. [5], [6] and references therein). Most recent works as Schury et al. [7], an efficient hierarchical topology optimization procedure with manufacturable constraint was presented. A design methodology for optimal poroelastic actuators was proposed by Andreasen et al. [8]. One should notice that the multiscale optimization methods mentioned above are actually a micro-/meso-scale material structure design optimization problem using macro-scale objective function. However, higher material savings and increased performance may be achieved if the structure and the cellular topologies are concurrently optimized.
Multi-scale design of structural and material has been considered with the use of porous materials in the seminal work by Bendsøe et al [9]. In their work, the recommended strategy was to consider simple square voids at the micro-scale in the context of minimum compliance design. Similar approach was extended to compliant mechanism design by Nishiwaki et al [10]. Rodrigues et al. [11] proposed a hierarchical

topology optimization method in which the micro-structure was no longer limited to a specific type (e.g., rectangular or square hole or ranked laminates). The proposed method was based on Free Material Optimization (FMO) [12] and an iterative approach presented by Theocaris et al [13], it decoupled the topology optimization into two related sub problems. The drawback of this methodology is that it contains sub problems which need to be solved that will lower efficiency of optimization procedure. Based on the works of Rodrigues [11], hierarchical topology optimization with similar approach had been extended on many different areas including minimization a compliance problem for 3D [14] and bone remodeling [15] were proposed by Coelho. More recent publications in multiscale topology optimization address multiscale topology optimization assuming a periodic cellular meso-structure, for which the periodic homogenization approaches were well established [16]. The optimum structures and material meso-structures for minimum compliance were achieved simultaneously. This method was further developed by Niu et al [17] working on the structure with optimum dynamic performance with maximum structural fundamental frequency, multi-objective concurrent topology optimization of thermoelastic structures by Deng et al [18], and also on compliant mechanism synthesis by Liu et al [19].
In our previous work [19], a design methodology for obtaining optimal macro-scale structures and the corresponding optimal meso-scale periodic material design in continuum design was proposed. The meso-structure is considered uniform on macro-scale. The objective of this investigation is to develop a multiscale approach for material and structural topology optimization relaxing the periodicity condition. The present work is an attempt to explore the optimal range for using non-periodic materials. However, this range changes corresponding to different problems. The resulting structures correspond to the optimal distribution of meso-structures of highest material saving. Since no preconceived meso and macrostructures are considered, the proposed multiscale topology optimization approach drives the design to non-intuitive configurations at both length-scales. The proposed approach makes use of homogenization techniques to make the multiscale analysis numerically tractable. This method is evaluated in the realms of minimum compliance and compliant mechanism problems, and compared to more traditional homogeneous and cellular material designs.

4. Problem Statement

The method incorporated in this paper is derived from the one originally introduced by [11]. The topology optimization problem is decoupled in two related sub-problems: structural design (macro) and material design (meso). The structural design problem aims to find the optimal material distribution on macroscopic level for a prescribed design domain and given boundary and loading conditions. The material design problem addresses the optimal material meso-structure of every macro-scale element. This methodology is not a classical topology optimization problem, but instead a multiscale (hierarchical) problem of structure and material design problem. This approach makes use of homogenization theory to establish communication bridges between both scales. While the effective properties of the meso-scale material are derived through homogenization, the analysis of objective function from the macro-scale structure required the effective properties of the meso-scale.

4.1. Formulation of the Optimization Problem on Macro-scale

An optimization problem on macro-scale including the features mentioned above can be written as:

$$
\begin{aligned}
&\text{find} \quad \mathbf{x} \\
&\min \quad F(\mathbf{x}, \mathbf{y}^1, \mathbf{y}^2, \ldots, \mathbf{y}^N) = \mathbf{F}^{\mathrm{T}}\mathbf{U} = \mathbf{U}^{\mathrm{T}}\ \mathbf{K}^{\mathrm{H}}(\mathbf{x}, \mathbf{y}^1, \mathbf{y}^2, \ldots, \mathbf{y}^N)\ \mathbf{U} = \sum_{i=1}^{N} \mathbf{U}_i^{\mathrm{T}}\ \mathbf{K}_i^{\mathrm{H}}(x_i, \mathbf{y}^i)\ \mathbf{U}_i \\
&\text{s.t.} \quad \mathbf{K}^{\mathrm{H}}(\mathbf{x}, \mathbf{y^1}, \mathbf{y^2}, \ldots, \mathbf{y^N})\ \mathbf{U} = \mathbf{F} \\
&\qquad \frac{V(\mathbf{x})}{V_\Omega} = \frac{\sum_{i=1}^{N} v_i x_i}{V_\Omega} = f \\
&\qquad 0 < \underline{x} \leqslant x_i \leqslant 1, \quad i = 1, \ldots, N
\end{aligned}
\tag{1}
$$

where $\mathbf{x}$ is the vector of macro-scale design variables (i.e. the element densities). $\mathbf{K}^{\mathrm{H}}$ is the homogenized global stiffness matrix dependent on two scales. $\mathbf{U}$ and $\mathbf{F}$ are the global displacement and force vector. $\mathbf{y}^i$ is the meso-scale design variables which will be discussed later. $V(\mathbf{x})$ and V_Ω are the material volume and design domain volume in macro-scale. N is the number of elements used to discretize the macro-scale design domain Ω. v_i and x_i are the element volume and density at macro-scale. f is the prescribed

volume fraction on macro-scale, respectively. $\underline{x}$ is a small number (1×10^{-3}) to avoid singularity in the stiffness matrix.

4.2. Formulation of the Optimization Problem on Meso-scale

From Eq.(1), the objective function, i.e. structure compliance, is the submission of every elements' compliance in the macro-scale. Apparently, the structure compliance can be minimized if the elements' compliance are minimized. In the spirit of this, we take advantage of topology optimization methods to find the morphologies of meso-structure.

Given the element displacement vector $\mathbf{U}_i$ and element density x_i at each spatial point i on macro-scale, we want to minimize the element compliance. Therefore, the meso-scale topology optimization problem for each spatial point i on macro-scale with density x_i can be stated as below

$$\begin{aligned} &\text{given} && \mathbf{U}_i, x_i \\ &\text{find} && \mathbf{y}^i \\ &\min && f(\mathbf{y}^i) = \mathbf{U}_i^{\mathrm{T}}\ \mathbf{K}_i^{\mathrm{H}}(x_i, \mathbf{y}^i)\ \mathbf{U}_i \\ &\text{s.t.} && \text{meso-scale equilibrium equations} \\ & && \frac{V(\mathbf{y}^i)}{V_Y} = \frac{\sum_{j=1}^{n} v_j y_j^i}{V_Y} = x_i \\ & && 0 < \underline{y} \leqslant y_j \leqslant 1, \quad j = 1, \ldots, n \end{aligned} \tag{2}$$

Here, the equilibrium equations on meso-scale of a unit base cell are given by the classic topology optimization method which will be discussed later. V_Y is the design domain volume in the meso-scale.

5. Numerical Implementation Issues

This section describes the numerical implementation of the proposed multi-scale topology optimization problem including initialization, homogenization, finite element discretization and procedures, sensitivity analysis, etc. A flow chart of the proposed design algorithm is shown in Fig. 1 and each individual step of the algorithm is described in the following.

5.1. Initialization

First we discretize the macro-scale design domain Ω into N elements and meso-scale design domains Y_i into n elements. Define the boundary conditions and loading conditions of structure. Provide base material properties Young's modulus: E_0 and Poisson's ratio ν.

5.2. Initial Design

The initial points of design variables in macro-scale $\mathbf{x}^{(0)}$ can be set uniform with value of macro-scale volume fraction f. The initial design variables for meso-scale problems $[\mathbf{y^i}]^{(0)}$ must start with a random density distribution. The initial uniform design variables (homogeneous material) would cause the gradients related to all design variables in meso-scale to have equal values, and thus, the optimization approach would not have a good direction for beginning the search. The final results are highly dependent on the initial design variables [3]. However, a considerable amount of computing time is saved by using good initial points.

In order to provide good initial points to the program, we are solving a small multiscale topology optimization problem and using the results as the starting points. This algorithm can be summarized below:

Step 1. A traditional macro-scale topology optimization problem is carried out with same boundary conditions, loading conditions, mesh size and material properties as we defined in the initialization step. Since there is no penalization method applied on the macro-scale, the objective function is a convex function which ensures the final results are the global minimum.

Step 2. A total number of N meso-scale optimization problems are solved to find the optimal meso-structure corresponding to the macro-scale solution in *Step 1.*

5.3. Homogenization

From the knowledge of finite element, the $\mathbf{K}_i^{\mathrm{H}}(x_i, \mathbf{y}^i)$ in Eq.(1) can be calculated through:

$$\mathbf{K}_i^{\mathrm{H}}(x_i, \mathbf{y}^i) = \int_{\Omega_i} \mathbf{B}^{\mathrm{T}} \cdot x_i [\mathbf{D}^{\mathrm{H}}(\mathbf{y}^i)]^0 \cdot \mathbf{B}\ d\Omega \tag{3}$$

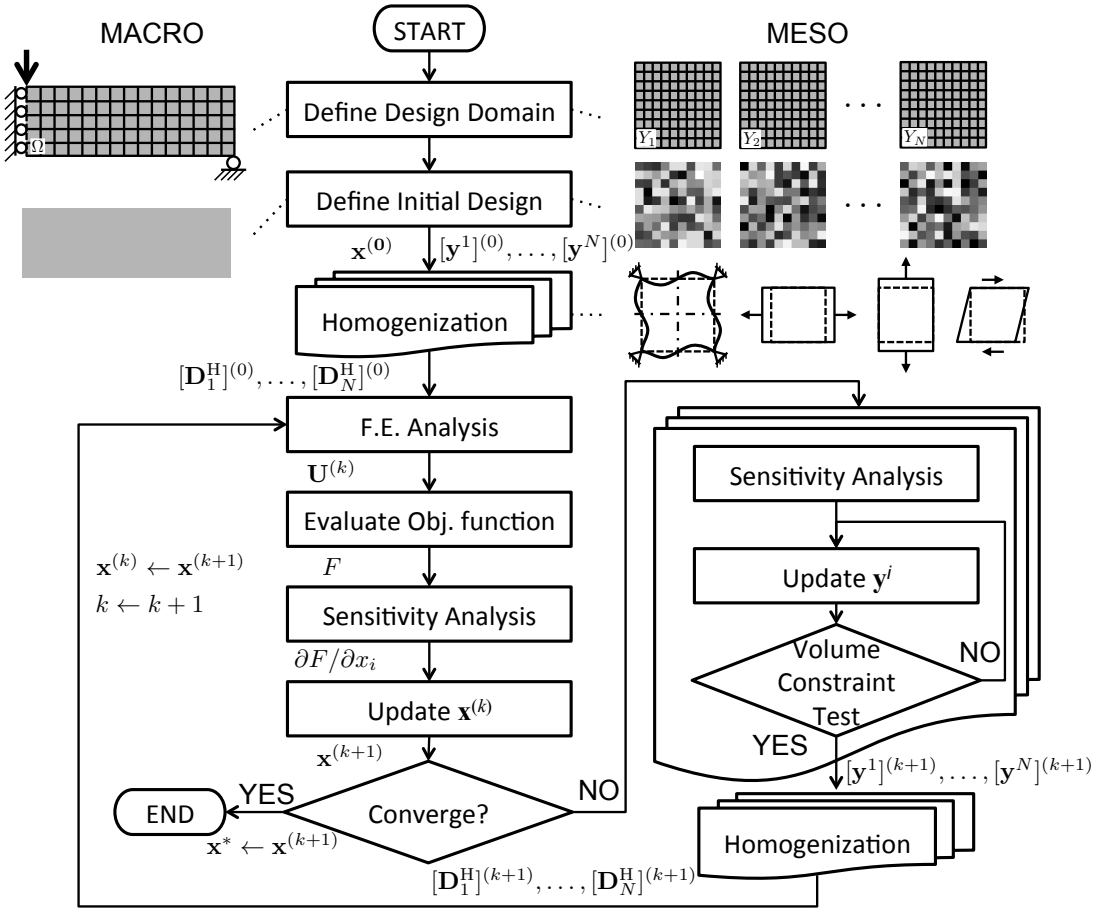

Figure 1: Programming flow chart

Here, $\mathbf{B}$ is the strain-displacement matrix at macro-scale, respectively. $[\mathbf{D}^{\mathrm{H}}(\mathbf{y}^i)]^0$ is the effective constitutive matrix with unit Young's modulus.
As mentioned before, the effective constitutive matrix $\mathbf{D}^{\mathrm{H}}$ is the key to connecting two scales: the effective material properties of meso-structure are represented by $\mathbf{D}^{\mathrm{H}}$, and this also related to the design of macro-structure as discussed above. The effective properties of meso-structure can be computed by following the standard homogenization theory [20].
The equilibrium equations of a unit cell are solved as a finite element problem with three different loading conditions which are special cases of unit initial strain loading

$$\mathbf{k}(\mathbf{y}^i)\ \mathbf{u}^{kl} = \mathbf{f}^{kl} \tag{4}$$

where the displacements $\mathbf{u}^{kl}$ $(k,l = 1,2$ for 2D problem) are constrained to be Y-periodic, as shown in Fig. 1, by either a penalty approach, Lagrange multipliers, or simply assigning equal node numbers to opposing boundary nodes [21]. The global stiffness matrix $\mathbf{k}$ in meso-scale is calculated as the usual assembly of element stiffness matrices $\mathbf{k}(\mathbf{y}^i) = \mathcal{A}_{j=1}^{n}\mathbf{k}_j(\mathbf{y}^i)$ plus corrections for periodicity.
The force vector is found from

$$\mathbf{f}^{kl} = \sum_{j=1}^{n}\int_{Y_j} \mathbf{b}^{\mathrm{T}} \cdot \mathbf{D}[\mathrm{E}_j^i(y_j^i)] \cdot \boldsymbol{\epsilon}^{0(kl)}\ dY \tag{5}$$

where $\mathbf{b}$ is the strain-displacement matrix in meso-scale. $\mathbf{D}[\mathrm{E}_j^i(y_j^i)]$ is the constitutive matrix in Hook's law with penalization (SIMP) as $\mathrm{E}_j^i(y_j^i) = (y_j^i)^\eta \mathrm{E}_0$, and $\boldsymbol{\epsilon}^{0(kl)}$ are the three cases of unit prestrain:

$$\boldsymbol{\epsilon}^{0(11)} = \begin{Bmatrix}1\\0\\0\end{Bmatrix} \qquad \boldsymbol{\epsilon}^{0(22)} = \begin{Bmatrix}0\\1\\0\end{Bmatrix} \qquad \boldsymbol{\epsilon}^{0(12)} = \begin{Bmatrix}0\\0\\1\end{Bmatrix} \tag{6}$$

Then, the effective material properties in finite element notation are computed via:

$$\mathbf{D}^{\mathrm{H}}_{ijkl}(\mathbf{y}^i) = \frac{1}{|Y|}\sum_{j=1}^{n}(\mathbf{u}^{0(ij)} - \mathbf{u}^{ij})^{\mathrm{T}} \int_{Y_j} \mathbf{b}^{\mathrm{T}}\ \mathbf{D}[\mathrm{E}^i_j(y^i_j)]\ \mathbf{b}\ dY\ (\mathbf{u}^{0(kl)} - \mathbf{u}^{kl}) \tag{7}$$

Note that for brevity of notation, we omitted the dependence of $\mathbf{D}^{\mathrm{H}}_{ijkl}$ on $\mathbf{u}$. Here, $|Y|$ is the volume (area in 2D) of a unit cell. $\mathbf{u}^{0(kl)}$ are the displacements corresponding to the test strains.

5.4. Sensitivity Analysis

The sensitivity of objective function F in macro-scale with respect to the design variable x_i can be easily found as

$$\frac{\partial F}{\partial x_i} = -\mathbf{U}_i^T\ \mathbf{K}^{\mathrm{H}}_i(\mathbf{y}^i)\ \mathbf{U}_i \tag{8}$$

The derivative of objective function f in meso-scale with respect to the design variable y^i_j is expressed as:

$$\begin{aligned}\frac{\partial f}{\partial y^i_j} &= -\mathbf{U}_i^T\ \frac{\partial \mathbf{K}^{\mathrm{H}}_i(x_i, \mathbf{y}^i)}{\partial y^i_j}\ \mathbf{U}_i \\ &= -\mathbf{U}_i^{\mathrm{T}}\left[\int_{\Omega_i} \mathbf{B}^{\mathrm{T}} \cdot x_i \frac{\partial[\mathbf{D}^{\mathrm{H}}(\mathbf{y}^i)]^0}{\partial y^i_j} \cdot \mathbf{B}\ d\Omega\right]\ \mathbf{U}_i\end{aligned} \tag{9}$$

and the sensitivity of a component of the effective constitutive matrix Eq.(7) with respect to the density design variable y^i_j can be found by the adjoint method. The resulting sensitivity expression in finite element notation is

$$\frac{\partial[\mathbf{D}^{H}_{ijkl}(\mathbf{y}^i)]^0}{\partial y^i_j} = \frac{1}{|Y|}\eta\big(y^i_j\big)^{\eta-1}(\mathbf{u}^{0(ij)} - \mathbf{u}^{ij})^{\mathrm{T}} \int_{Y_j} \mathbf{b}^{\mathrm{T}}\ \mathbf{D}_0\ \mathbf{b}\ dY(\mathbf{u}^{0(kl)} - \mathbf{u}^{kl}) \tag{10}$$

where $\mathbf{D}_0$ is the constitutive matrix with unit Young's modulus.

5.5. Optimum Search and Convergence

As the optimizer, we use the MATLAB implementation of the Method of Moving Asymptotes (MMA) [22] made freely available for research purposes by Krister Svanberg. The iterative design approach is repeated until the change in each design variables in two successive iterations is less than 0.01.

5.6. Regularization Techniques

The standard 'density approach to topology optimization' [1] is likely to encounter problems with mesh-dependency and checkerboard pattern if no regularization techniques are applied. In order to avoid numerical instabilities, we introduced the classic density filter to our implementation. Density filter first introduced by Bruns et al. [23] and further proved mathematically by Bourdin et al. [24] has become a usual regularization scheme in SIMP based topology optimization procedure. The standard density filter given as

$$\tilde{X}_e = \frac{\sum \omega\ v_e\ X_e}{\sum \omega\ v_e} \tag{11}$$

where v_e and X_e denotes the volume and density of design variable e. For example, in macro-scale, $v_e = v_i$ and $X_e = x_i$, and in meso-scale, $v_e = v_j$ and $X_e = y^i_j$. ω is the weight factor, and it is given by a linear function as suggested in [23]

$$\omega = \max\{0,\ r_{\min} - \mathrm{dist}(e,h)\}, \quad \{h \in N(\text{or } n) \mid \mathrm{dist}(e,h) \leqslant r_{\min}\} \tag{12}$$

where the operator $\mathrm{dist}(e,h)$ is defined as the distance between center of element e and center of element h. $r_{\min}$ is the radius (or filter size).

5.7. Discontinuities

If the meso-structure is assumed identical over macro-scale, there is normally no connection problem between adjacent elements on macro-scale level because the unit cell is imposed with periodic boundary conditions (Fig. 1). However, in our study, the meso-structures vary pointwise. From numerical experiments, discontinuities exist between adjacent elements. To address this problem, we proposed a method

which converts the distributed load on meso-scale boundaries to 2 concentrated loads on each boundary. This method is illustrated in Fig. 2a. Figure 2b shows the two optimized topologies for different loading cases. There are some differences shown in the meso-structures of two loading cases; more obvious differences can be found by increasing the finite element mesh size of macro-scale design domain.

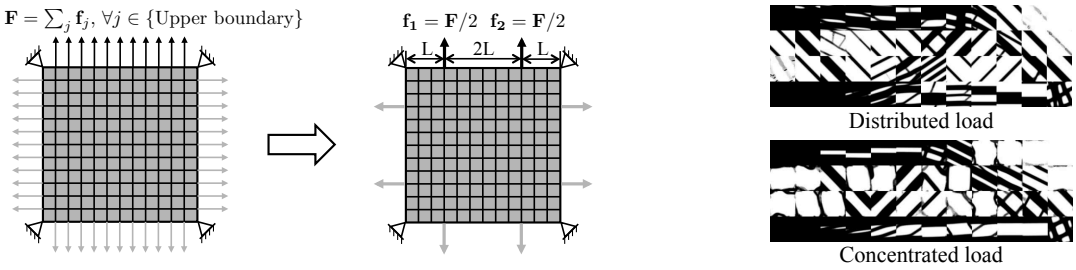

(a) Distributed load to Concentrated load.

(b) Resulting topologies for different loading cases.

Figure 2: Strategy of solving discontinuities issue.

6. Numerical Examples

In order to demonstrate the effectiveness of the proposed method for minimum compliance design, we solve a classic and well-known MBB-beam problem. In addition, a widely used Force inverter with maximum output displacement is solved, which indicates the effectiveness of our proposed method in compliant mechanism.

6.1. MBB-beam

A classic MBB-beam problem with a concentrated vertical force of $F = 1$ is loaded at center of the top edge and the structure is supported horizontally in the lower right corner. Only half of the MBB-beam is considered due to the axial symmetry, and the macro-scale design domain is sketched as shown in Fig. 3a. The macro-scale design domain is discretized into 60×20 elements. The structure volume fraction f is prescribed to be 0.50. The base material has Young's modulus $E_0 = 1.00$ and Poisson's ratio $\nu = 0.30$. The filter size of macro-scale is 0.03 times the width of the design domain and 0.04 times the width of meso-scale design domain.

6.1.1. Meso-scale mesh size effect

The main objective of this example is to analyze the influence of the mesh size for the meso-scale design domain in the overall structure topologies and in the objective function. As reference, the topology for the homogeneous material is shown in Fig. 3b with objective value 207.8551. The meso-scale design domains have different mesh sizes with 20×20, 30×30, 40×40, 50×50, and 60×60 finite elements. Some selective topologies are shown in Fig. 4. As it can be seen from Fig. 4, the connection between adjacent elements in macro-scale is smoother with the increasing of mesh size of meso-scale. Figure 4 shows the final topologies are mesh-independent, which means the differences between different meso-scale design domain mesh sizes are minor. However, the meso-structures are quite different in different mesh sizes. As predicted, as the discretization of the meso-scale design domain increases, there is an improvement on the overall structural performance.

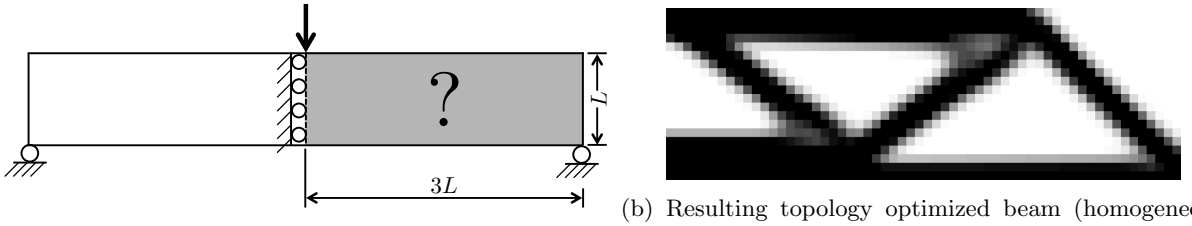

(a) Initial design domain for MBB-beam.

(b) Resulting topology optimized beam (homogeneous materials).

Figure 3: Initial design domain for MBB-beam and its reference solution.

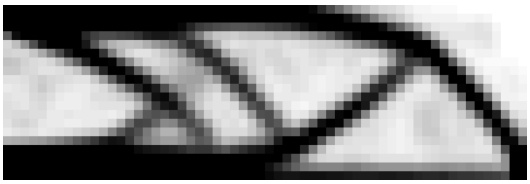

(a) Macro-scale density distributions (20×20).

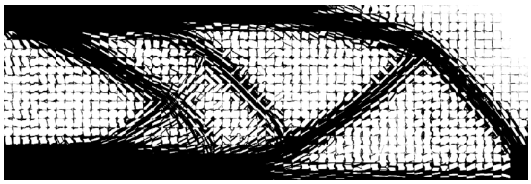

(b) Resulting topology optimized beam (20×20).

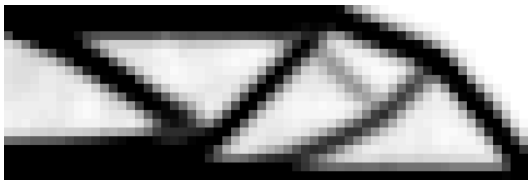

(c) Macro-scale density distributions (60×60).

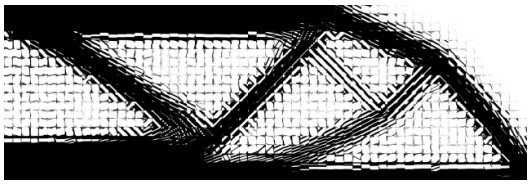

(d) Resulting topology optimized beam (60×60).

Figure 4: Selective results for MBB-beam.

6.1.2. Periodic vs. non-periodic vs. homogeneous

In our previous work [19], we found that the structures with periodic cellular materials on macro-scale level cannot completely replace the homogeneous materials especially when higher structural performances are required. However, cellular materials can be used to achieve ultra-lightweight structure with clear black-and-white topologies. In this example, we want to compare the structural performance with structures using periodic cellular materials, non-periodic cellular materials and homogeneous materials. The details of the problem setting can be found in [19]. For the non-periodic problem, the macro-scale design domain is discretized into 30×10 elements, and meso-scale design domain is discretized into 20×20 elements. The pareto fronts are shown in Fig. 6. Speaking to the structural performances as shown in Fig. 6, non-periodic materials have lower compliance compared to the periodic materials. However, when mass fractions are bigger than 0.25, the structures with homogeneous materials are more preferable (for details c.f. [19]) if we combine the structure performance with computing time.

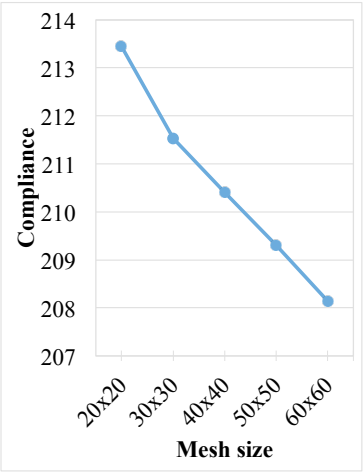

Figure 5: Compliance versus mesh size.

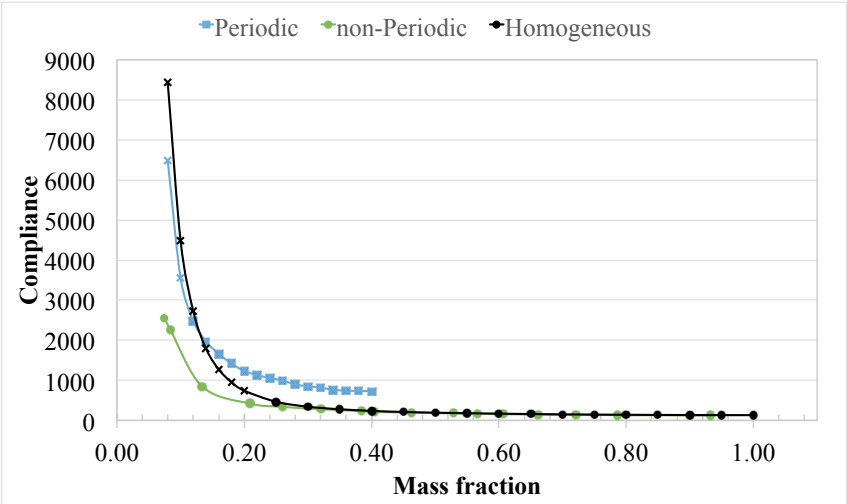

Figure 6: Pareto fronts of MBB-beam

6.2. Force Inverter

A compliant mechanism is a morphing structure that undergoes elastic deformation to transform force, displacement, or energy. One of the main advantages of considering compliant mechanisms is the dramatic reduction in the number of components required for the specific task. Compliant mechanisms naturally store elastic energy and they can be considered as an alternative to rigid body linkages that

incorporate springs. Mechanical and geometric advantages can be considered in compliant mechanism optimization [25].
In compliant mechanism synthesis, a typical objective is to maximize output port displacement. The objective function can be found through the dummy load method

$$F(\mathbf{x}) = -u_{out} = -\mathbf{L}^{\mathrm{T}}\mathbf{U} = \boldsymbol{\lambda}^{\mathrm{T}}\ \mathbf{K}^{\mathrm{H}}(\mathbf{x}, \mathbf{y}^1, \mathbf{y}^2, \ldots, \mathbf{y}^N)\ \mathbf{U} \tag{13}$$

where $\boldsymbol{\lambda}$ refers to the global adjoint vector in macro-scale which can be found by the solution of the adjoint problem: $\mathbf{K}^{\mathrm{H}}(\mathbf{x}, \mathbf{y}^1, \mathbf{y}^2, \ldots, \mathbf{y}^N)\ \boldsymbol{\lambda} = -\mathbf{L}$.
The design domain for the force inverter example is sketched in Fig. 7a. The goal is the maximization of the output displacement in the negative horizontal direction due to an input load of $f_{in} = 1$ in the positive direction. Due to symmetry, the lower half of the design domain has modeled and discretized into 50×25 elements, and the meso-scale design domain is discretized into 20×20 elements. The structure volume fraction f is predefined to 0.30. The filter size of macro-scale is 0.03 times the width of the design domain ($50 \times 0.03 = 1.50$), and 0.04 times the width of meso-scale design domain ($20 \times 0.04 = 1.20$). The input and output springs have a stiffness of 0.01 and 0.01.The base material has Young's modulus $\mathrm{E}_0 = 1.00$ and Poisson's ratio $\nu = 0.30$.
Solving the small initial topology optimization problem as stated earlier in compliant mechanism problem is not required, since the objective function of compliant mechanism is not convex, which means it cannot guarantee the local minima is the global minima. The initial macro-scale design variables $\mathbf{x}^0$ are uniform with value of macro-scale volume fraction f. The initial design variables for meso-scale $[\mathbf{y}^i]^{(0)}$ must start with a random density distribution and the final results are highly dependent on the initial design variables.
The optimized topology is shown in Fig. 8. Comparing the topologies with the reference solution as shown in Fig. 7b, the macro-scale structures are quite similar. However, a hinger exists in the multiscale optimized structure. The pareto fronts of periodic cellular materials, non-periodic cellular materials and homogeneous materials are shown in Fig. 9. In Fig. 9, similar conclusion can be derived as minimum compliance problem, and non-periodic cellular materials show more gains than periodic cellular materials in compliant mechanism problems. Comparing with the minimum compliance problem, there are more availabilities of using non-periodic cellular materials. The trend of pareto front of non-periodic material is similar with the trend of homogeneous materials. When mass fraction is over 0.35, using homogeneous materials is more recommended due to the lower computational cost and higher structural performance.

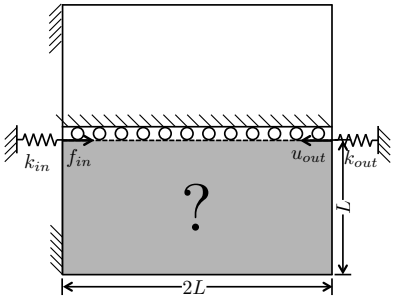

(a) Initial design domain for force inverter.

(b) Resulting topology optimized force inverter (homogeneous materials).

Figure 7: Initial design domain for force inverter and its reference solution.

7. Conclusions

Multiscale topology optimization methodologies using non-periodic cellular materials for minimum compliance problem and synthesizing compliant mechanisms were proposed. Comparisons between using periodic materials, non-periodic materials and homogeneous materials were presented in this work.
Numerical results shows that homogeneous material cannot be replaced by cellular materials when high structural performance is desired. However, using cellular materials with low mass fractions are better than using homogeneous materials. Those structures in the ultra-light structures with cellular materials have better structural performance and less structure mass than the homogeneous materials. In both minimum compliance and compliant mechanism problems, the usage of non-periodic cellular materials are naturally superior to the periodic cellular materials in the ultra-light structure (low mass fraction) ranges.

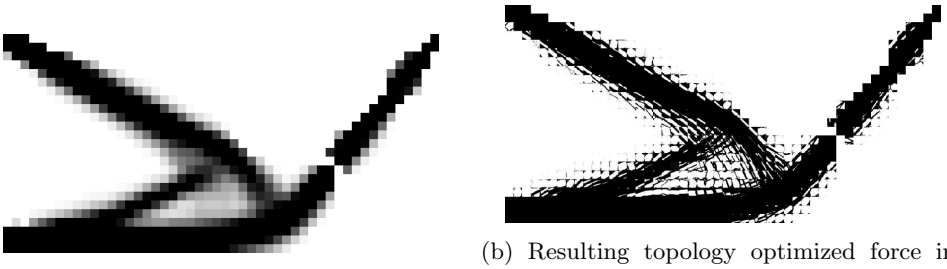

(a) Macro-scale density distributions.

(b) Resulting topology optimized force inverter.

Figure 8: Selective results for force inverter.

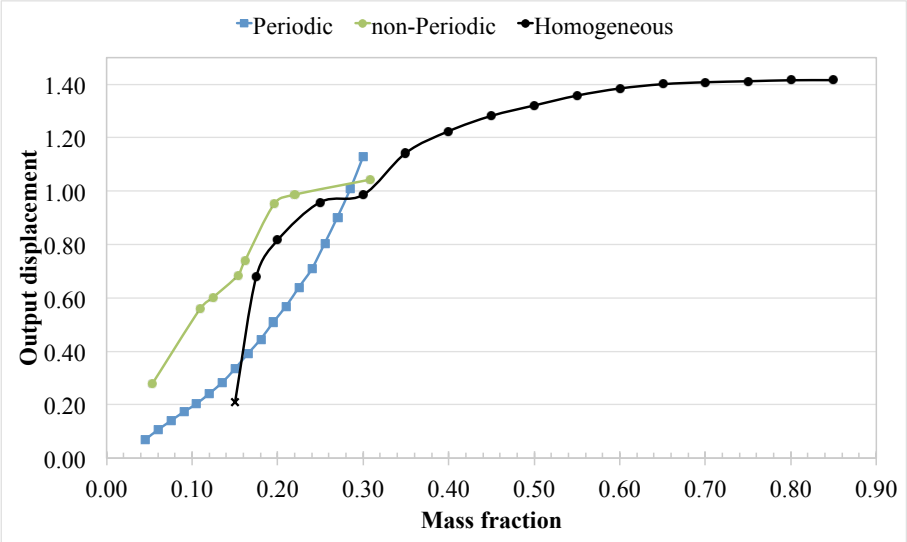

Figure 9: Pareto fronts of force inverter

However, one should notice that those ranges are various based on different problems. The benefits of using non-periodic cellular materials in compliant mechanism design problems are more obvious than the minimum compliance.
The superiorities of using cellular materials with high mass fraction are limited under deterministic design if only the structural performances are compared. Even so, structures with cellular materials are always considered as multi-functional objectives. Furthermore, we believe that the cellular materials will perform much better than the homogeneous materials under uncertainty which will be the next step of this work.

8. References

[1] M. P. Bendsøe, "Optimal shape design as a material distribution problem," *Struct Multidisc Optim*, vol. 1, no. 4, pp. 193–202, 1989.

[2] J. M. Guedes and N. Kikuchi, "Preprocessing and postprocessing for materials based on the homogenization method with adaptive finite element methods," *Comput. Methods Appl. Mech. Eng.*, vol. 83, no. 2, pp. 143 – 198, 1990.

[3] O. Sigmund, "Materials with prescribed constitutive parameters-an iverse homogenization problem," *Int J Solids Struct*, vol. 31, no. 17, pp. 2313–2329, 1994.

[4] G. H. Paulino, E. C. N. Silva, and C. H. Le, "Optimal design of periodic functionally graded composites with prescribed properties," *Struct Multidisc Optim*, vol. 38, no. 5, pp. 469 – 489, 2009.

[5] M. P. Bendsøe, L. Erik, and O. Niels, "Topology optimization-broadening the areas of application," *Control and Cybernetics*, vol. 34, pp. 7–35, 2005.

[6] J. E. Cadman, S. Zhou, Y. Chen, and Q. Li, "On design of multi-functional microstructural materials," *Journal of Materials Science*, vol. 48, no. 1, pp. 51 – 66, 2013.

[7] F. Schury, M. Stingl, and F. Wein, "Efficient two-scale optimization of manufacturable graded structures," *SIAM Journal on Scientific Computing*, vol. 34, no. 6, pp. B711 – B733, 2012.

[8] C. Andreasen and O. Sigmund, "Multiscale modeling and topology optimization of poroelastic actuators," *Smart Mater. Struct.*, vol. 21, 2012.

[9] M. P. Bendsøe and N. Kikuchi, "Generating optimal topologies in structural design using a homogenization method," *Comput. Methods Appl. Mech. Eng.*, vol. 71, no. 2, pp. 197–224, 1988.

[10] S. Nishiwaki, M. I. Frecker, S. Min, and N. Kikuchi, "Topology optimization of compliant mechanisms using the homogenization method," *Int J Numer Methods Eng*, vol. 42, pp. 535–559, 1998.

[11] H. Rodrigues, J. Guedes, and M. P. Bendsøe, "Hierarchical optimization of material and structure," *Struct Multidisc Optim*, vol. 24, no. 1, pp. 1–10, 2002.

[12] J. Zowe, M. Kočvara, and M. P. Bendsøe, "Free material optimization via mathematical programming," *Mathematical Programming*, vol. 79, no. 1-3, pp. 445–466, 1997.

[13] P. Theocaris and G. Stavroulakis, "Optimal material design in composites: An iterative approach based on homogenized cells," *Comput. Methods Appl. Mech. Eng.*, vol. 169, no. 1-2, pp. 31 – 42, 1999.

[14] P. Coelho, P. Fernandes, J. Guedes, and H. Rodrigues, "A hierarchical model for concurrent material and topology optimisation of three-dimensional structures," *Struct Multidisc Optim*, vol. 35, no. 2, pp. 107 – 115, 2008.

[15] P. Coelho, P. Fernandes, H. Rodrigues, J. Cardoso, and J. Guedes, "Numerical modeling of bone tissue adaptation-a hierarchical approach for bone apparent density and trabecular structure," *Journal of Biomechanics*, vol. 42, no. 7, pp. 830 – 837, 2009.

[16] L. Liu, J. Yan, and G. Cheng, "Optimum structure with homogeneous optimum truss-like material," *Comput Struct*, vol. 86, no. 13-14, pp. 1417–1425, 2008.

[17] B. Niu, J. Yan, and G. Cheng, "Optimum structure with homogeneous optimum cellular material for maximum fundamental frequency," *Struct Multidisc Optim*, vol. 39, pp. 115–132, 2009.

[18] J. Deng, J. Yan, and G. Cheng, "Multi-objective concurrent topology optimization of thermoelastic structures composed of homogeneous porous material," *Struct Multidisc Optim*, pp. 1 – 15, 2012.

[19] K. Liu and A. Tovar, "Multiscale topology optimization of structures and cellular materials for compliant mechanism design," in *Proceedings of the ASME 2013 International Design Engineering Technical Conferences and Computers and Information in Engineering Conference*, 2013.

[20] M. P. Bendsøe and O. Sigmund, *Topology optimization: theory, method and applications*, 2nd, Ed. Springer, 2003.

[21] R. Cook, D. Malkus, and M. Plesha, *Concepts and application of finite element analysis*, 3rd, Ed. Wiley, 1989.

[22] K. Svanberg, "The method of moving asymptotes-a new method for structural optimzation," *Int J Numer Methods Eng*, vol. 24, pp. 359–373, 1987.

[23] T. Bruns and D. Tortorelli, "Topology optimization of non-linear elastic structures and compliant mechanisms," *Comput. Methods Appl. Mech. Eng.*, vol. 190, no. 26-27, pp. 3443–3459, 2001.

[24] B. Bourdin, "Filters in topology optimization," *Int J Numer Methods Eng*, vol. 50, no. 9, pp. 2143–2158, 2001.

[25] M. Y. Wang, "Mechanical and geometric advantages in compliant mechanism optimization," *Frontiers of Mechanical Engineering in China*, vol. 4, no. 3, pp. 229–241, 2009.